Report no. changed (Mar 2006): SM-391-UU

SACLANTCEN MEMORANDUM
serial no: SM- 391

SACLANT UNDERSEA RESEARCH CENTRE REPORT

Noise measurements during MAPEX2000

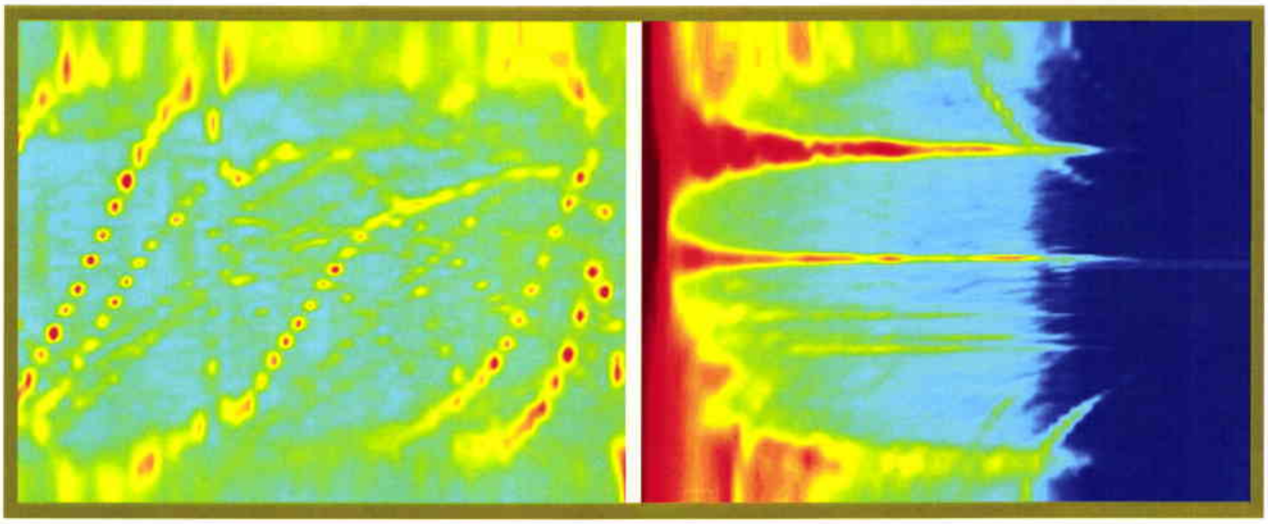

Chris H. Harrison

March 2002

NORTH ATLANTIC TREATY ORGANIZATION ORGANISATION DU TRAITE DE L'ATLANTIQUE NORD

Noise measurements during MAPEX2000

C.H. Harrison

The content of this document pertains to work performed under Project 01-B of the SACLANTCEN Programme of Work. The document has been approved for release by The Director, SACLANTCEN.

Jan L. Spoelstra
Director

intentionally blank page

Noise measurements during MAPEX2000

C.H. Harrison

Executive Summary: Both passive and active sonars may have their detection ranges restricted by the ambient noise of wind and shipping. Therefore it is important not only to know the current, local noise levels and directionalities, but to be able to predict values at other locations in the battlespace. The possibility of using satellite Synthetic Aperture Radar (SAR) imagery to predict shipping and wind and thereby noise was investigated during the MAPEX2000 experiment on the Malta Plateau in March 2000. Satellite SAR images were collected simultaneously with horizontal array (HLA) ambient noise measurements. This report completes all the acoustic analysis of the horizontal array data for two days during the experiment, in which weather was first relatively good then extremely bad. Comparisons with satellite data are addressed in a separate report.

Over several hours one can see many passing ships in the beam-formed sonar records. As one would expect, there are significant differences in the number of ships detected on the calm and the rough day. This is partly due to propagation effects, but also due to the reduction in density of shipping in such heavy seas.

By looking at the maximum and minimum noise level over a period of hours, for each beam and frequency, it is possible to separate the noise of local individual ships from the (angle- and frequency-dependent) smooth background of distant shipping.

As a by-product it was possible to check the spectra of individual ships and to investigate the aspect-dependence of their radiated noise as they passed.

intentionally blank page

Noise measurements during MAPEX2000

C H Harrison

Abstract: During MAPEX2000 some simultaneous ambient noise measurements with an HLA and satellite SAR images were collected. The aim was to predict shipping and wind noise from the satellite radar and to compare results with acoustic measurements. This report takes the acoustic data alone and investigates differences in noise directionality and shipping densities in fair and rough weather conditions. Directionality and various statistics are studied as a function of frequency and time (several hours). In addition, picking one ship at a time it is possible to study its aspect dependence as it passes the HLA.

Keywords: Ambient noise, wind noise, shipping noise, beam-forming, HLA, noise directionality.

Contents

1
Introduction

During February and March 2000 a series of experiments called MAPEX2000 was carried out on the Malta Plateau between Sicily and Malta [1]. One of the objectives of these experiments was to test the idea that satellite SAR (synthetic aperture radar) images of shipping and sea surface roughness could be used to improve predictions of ambient noise. Towed array measurements of directional ambient noise were made over a period of several hours on two occasions, both coincident with the twice daily crossing of Radarsat. The intention of this report is to restrict attention to the noise measurements alone and any deductions that can be made from these without using models. In the meantime the extent to which ship size, position, speed, and heading can be deduced from satellite and MPA (marine patrol aircraft) data has been examined in [2]. A future report will compare modelled noise using satellite data with these measured results.

More specifically, noise measurements were collected with the 256 element towed HLA for 5 s every 5 min on one day (good weather) and 10 s every 10 min on the other (bad weather). Using frequency domain beamforming the data were reduced to a function of beam angle, frequency and time for the two days. By looking at the statistical behaviour of the several-second-average over hours (max, min, mean, median, etc) it is possible to separate the nearby individual ships from the more slowly varying background. Firstly one can make a number of deductions about individual ships (relating to their spectra and aspect dependence). Secondly one can deduce the smooth background spectrum versus angle. Surprisingly the minimum noise over the several hours, a frequency and angle dependent background, appears not to depend on weather. Thirdly it is possible to see the behaviour of the *Alliance's* self noise (hull slamming and associated wave and spray noise) in rough weather.

2
Experimental arrangement

Timing of the noise trial was predetermined by the crossings of Radarsat with suitable coverage at 16:50 on the 2nd March, 05:06 on the 3rd March, and 05:02 on the 10th March. The original intention was to start several hours before the satellite crossing and base the shiptrack on a large triangle with the second leg roughly parallel to the Sicilian coast and the main shipping lane from Gibraltar to the Suez Canal [3]. The idea was to be heading ESE towards the ridge of the Malta Plateau with aft endfire beam looking down the shipping lane. Unfortunately on the night of the 2nd March when the array was already out the weather was extremely bad with winds from the NW so that the only possibility was a run *towards* the NNW and then to abandon the run before the satellite crossing time. On the second day weather had improved and a single track to the ESE was completed with satellite crossing near the centre of the track.

The final ship tracks and the satellite crossing position are shown in Fig 1. The array heading was 292° towards WNW on the 3rd and 114° towards ESE on the 10th.

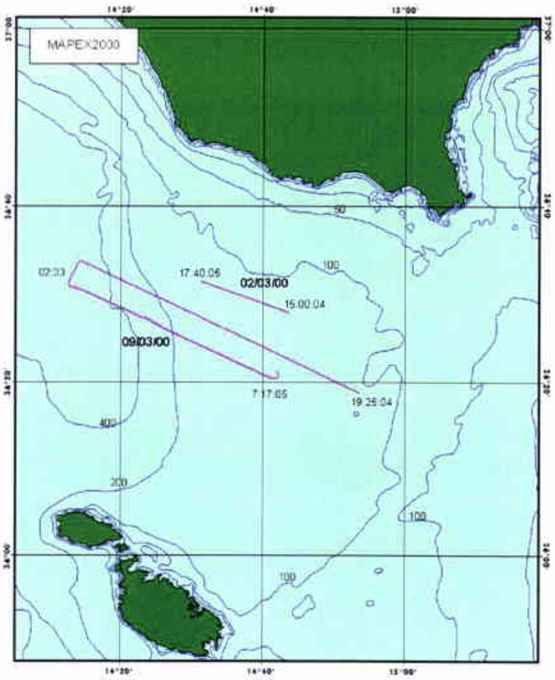

Figure 1 *Ship tracks south of Sicily.*

The 256 element HLA was towed (array centre at 640 m behind the ship's radar) at 40 to 60 m depth. The signal was sampled at 6 KHz. Anti-aliasing filters were set at 2 KHz and a high-pass filter with 6dB per octave roll-off [4] set at 100 Hz on the 3rd but 20 Hz on the 10th.

Although environmental data (CTD, XBT, bathymetry, geoacoustic parameters) are available they will not be presented here since we postpone modelling comparisons until a later report. In the meantime the waverider buoy wave height plot (Fig. 2) gives an idea of the difference between the 'rough' day and the 'calm' day.

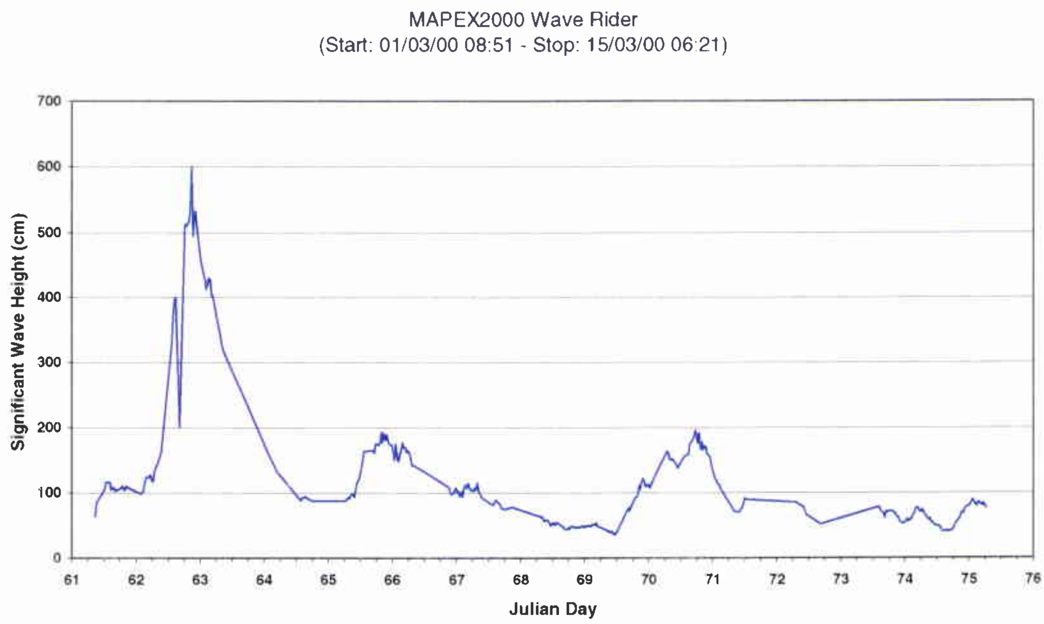

Figure 2 *Waverider wave height plot. Noise measurements were made on Julian days 62 and 69/70 (2nd and 9/10th March).*

3
Signal processing

3.1 Beam forming and spectral analysis

Beam forming is carried out in the frequency domain. The array response A for each beam can be written in terms of the cross spectral density matrix $\mathbf{R}$ and the steering vector $\mathbf{w}$ as

$$A(\theta_s) = \mathbf{w}^T \mathbf{R}\, \mathbf{w}$$

The steering vectors $\mathbf{w}$ are of the form

$$\mathbf{w} = w_n(\theta_s) = a_n \exp(-i\,k\,x_n \sin(\theta_s))$$

where θ_s is the steer angle, k is the wavenumber, x_n is distance along the array, and a_n is the shading (hamming) normalized so that the centre beam is unity. Incidentally this normalization has an important effect on noise. The response from a point source ('signal' or 'noise') in centre beam is always unaffected by the beam properties; distributed sources, however, produce more noise the wider the beam.

Given the time series for each hydrophone one could use the MATLAB function CSD to construct $\mathbf{R}$ by taking all pairs in turn. For large numbers of hydrophones it is numerically more efficient to calculate the array response from the Fourier transform $\mathbf{x}$ of the time series as

$$A(\theta_s) = \left|(\mathbf{w}^T \mathbf{x})\right|^2$$

which is exactly equivalent. The power response for non-overlapping 128-point FFTs was then averaged for the first 234 FFTs of the 5 or 10 second file (234×128 samples at 6KHz sampling take just under 5 seconds).

The result of this processing is 64 frequencies (0 to 3000Hz) up to Nyquist, but this is hardware filtered as well, as described above. Calculations were carried out for 181 angles (1° separation between –90° and 90°). Thus we have array response to noise as a function of steer angle, frequency and time.

The hydrophones are physically arranged with an inner group of 128 at 0.5 m spacing. There are a further 32 at each end with 1.0 m spacing, and outside this another set of 32 at each end with 2.0 m separation. When processing in the frequency domain it is possible to include more hydrophones at the lower frequencies (still within the design frequency) thus maximizing angle resolution at the lower frequencies. Unfortunately the frequency response is spoilt because there is typically a mixture of point sources and distributed sources; as mentioned earlier, a point source is unaffected because the beams are normalized, but the response to a distributed source falls roughly as 1/M with M hydrophones because of the narrowing of the beam with M. Nevertheless the difference is an interesting discriminant which is examined below. Otherwise all spectra use only the central 128 hydrophones.

4
Noise *versus* beam, frequency and time

4.1 Passing ships

The sequence of Figs. 3 (a,b,c,d) and 4 (a,b,c,d) give an overview of the behaviour of noise against all three parameters, angle, time and frequency. Figure 3 is for the calm day (10th March) and Fig. 4 is for the rough day (2nd March). In Fig. 3(a) we see beam formed data from the 52 files, one per 5 min, for 1 KHz. The main features are seven individual ships causing the 's' shaped brown and yellow curves as they overtake the *Alliance*, i.e. pass from endfire aft to endfire forward. A number of weaker ships can also be seen. This is superimposed on a more uniform spread of wind and distant shipping, although there is a stronger contribution in the two endfire directions than at broadside. Note that any ship on a constant heading will appear to the (moving) array as the line

$$\tan(\theta - \theta_{cpa}) = v(t - t_{cpa}) / r_{cpa}$$

where the subscripts refer to the point of closest approach. The only distinguishing feature of a ship on a parallel track to the array is that $\theta_{cpa} = \pi/2$ so the asymptotes of the tan are exactly fore and aft.

At lower frequencies, Figs. 3 (b,c,d), the most obvious point is that the resolution of the beams gets poorer. At 200 Hz the seven ships are still identifiable, and, in fact, two more can be seen at about 200 min passing in the opposite direction. At 100 Hz, though, most of these do not contribute and there remains a strong ship return at around 30 and 240 min.

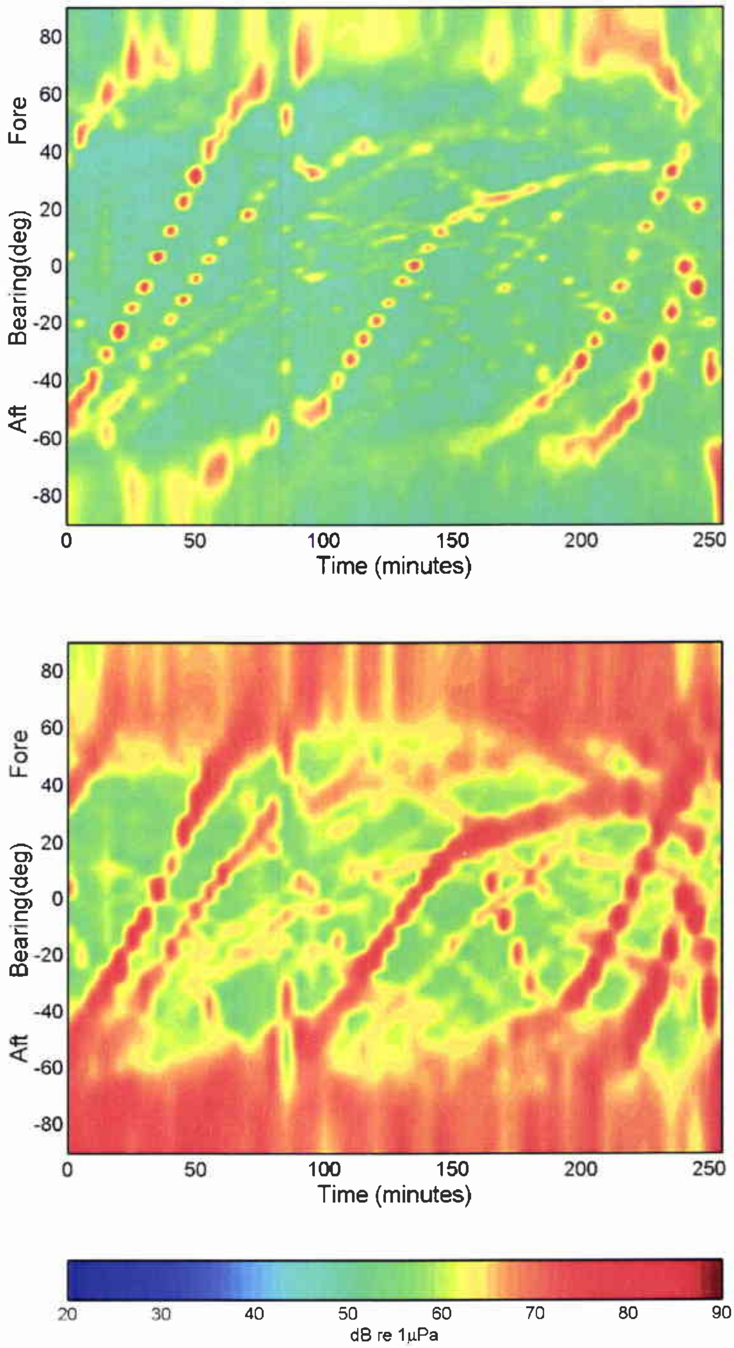

Figure 3 (a), (b) *Noise vs beam angle and time for the first and second of four frequencies (1000,500,200,100 Hz) on the calm day.*

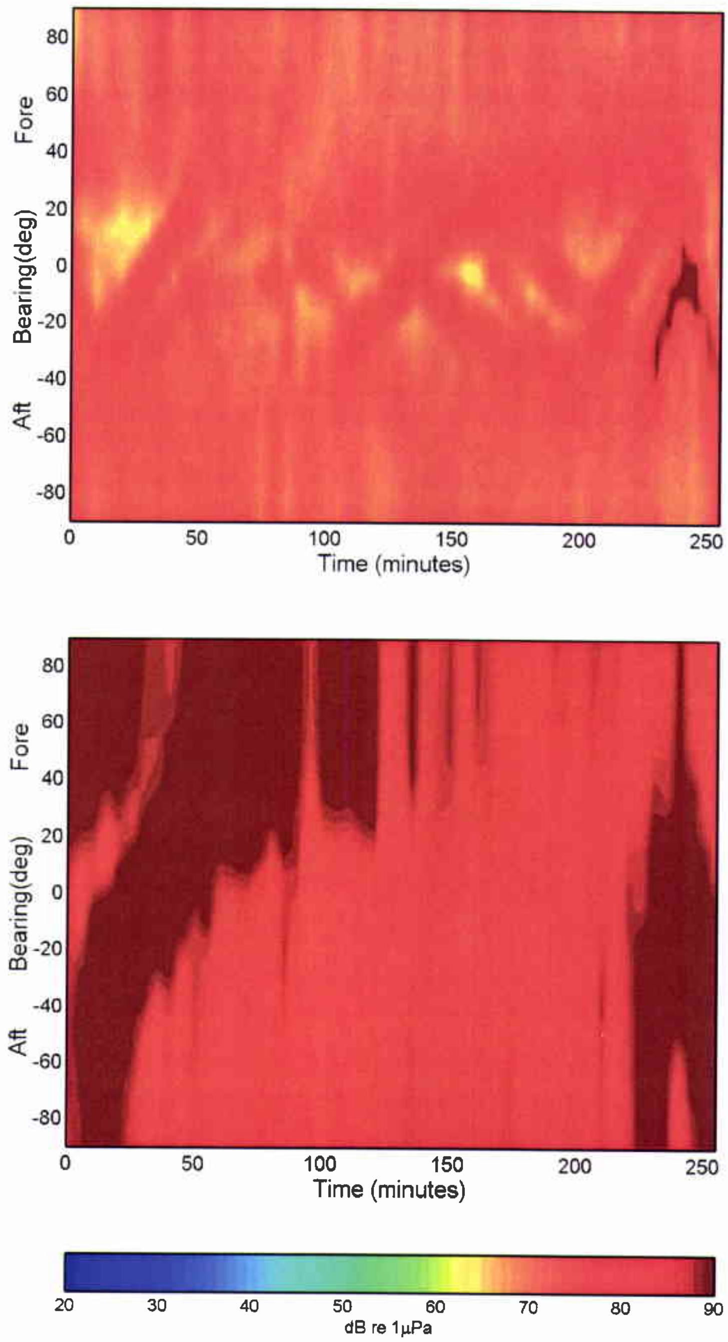

Figure 3 (c), (d) *Noise vs beam angle and time for the third and fourth of four frequencies (1000,500,200,100 Hz) on the calm day.*

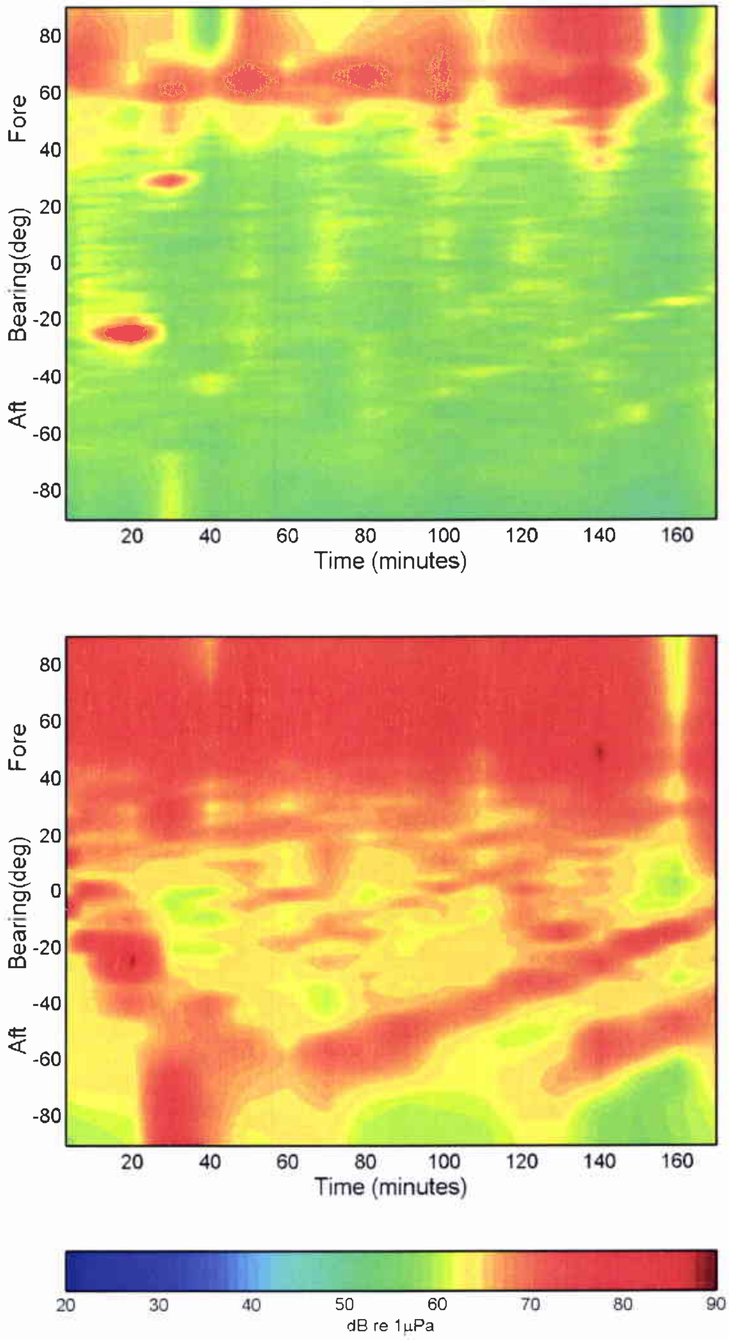

Figure 4 (a), (b) *Noise vs beam angle and time for the first and second of four frequencies (1000,500,200,100 Hz) on the rough day.*

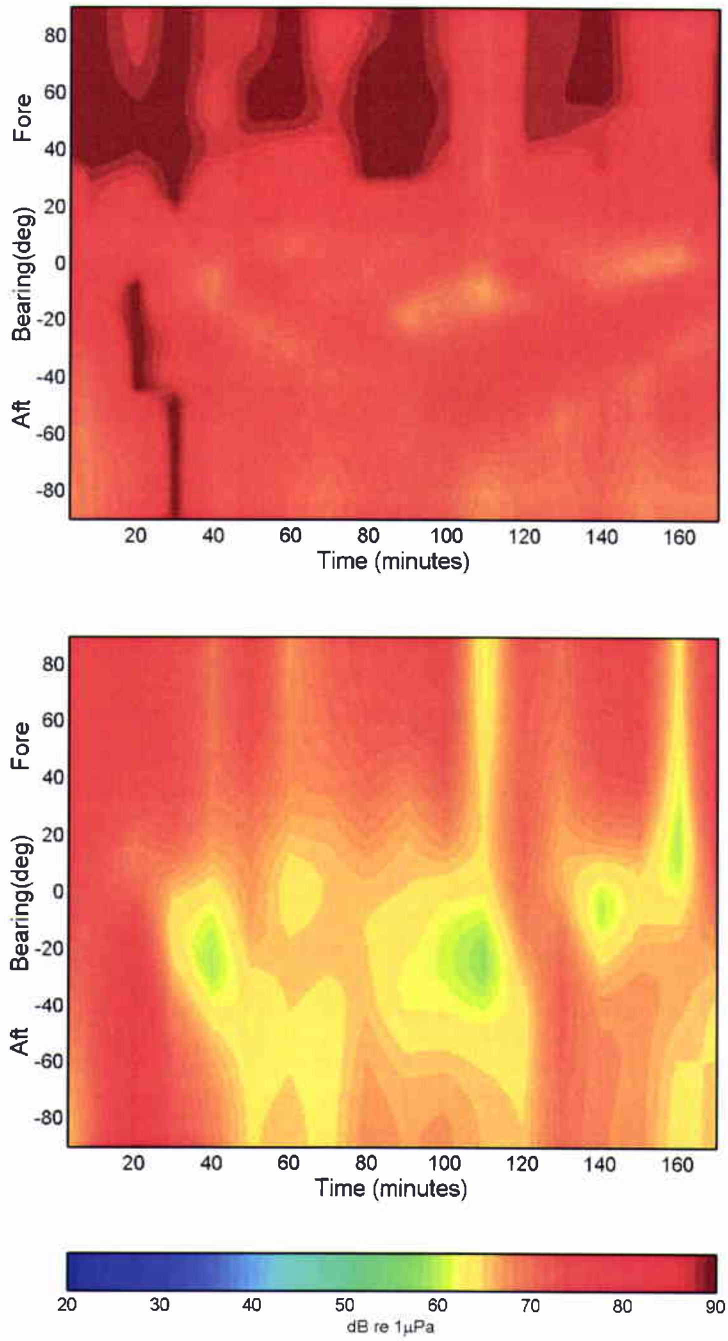

Figure 4(c) (d) *Noise vs beam angle and time for the third and fourth of four frequencies (1000,500,200,100 Hz) on the rough day.*

Comparing the equivalent picture for rough weather (Fig. 4 (a), 18 files, one per 10 min) we see that fewer ships are visible. In principle this could be because local wind noise masks them, or propagation is poor or there really are fewer ships. At the top of the picture is self noise in the endfire beam due to 'slamming' of the stern. Even the quiet ship *Alliance* cannot avoid making noise in bad weather. The view over the stern of the *Alliance* (Fig. 5 (a), (b)) and the waverider plot makes it clear that these are exceptional circumstances.

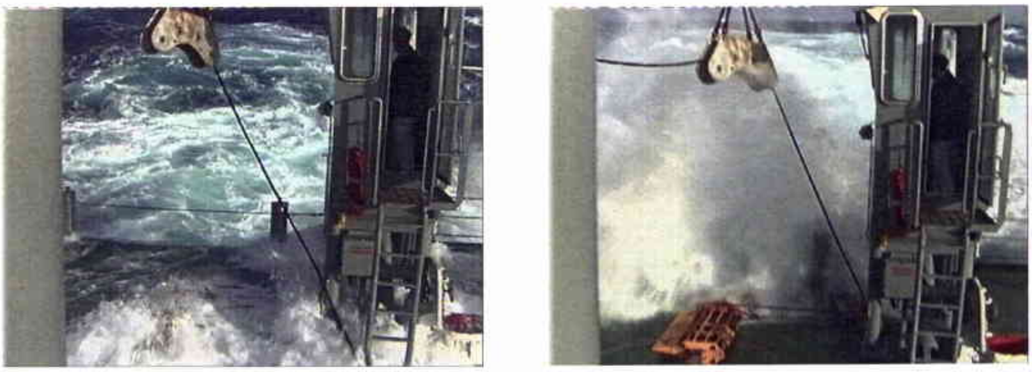

Figure 5 *Stern of the Alliance on 3^rd March 2000*

4.2 Beam response at a single frequency

An example of the beam formed spectrum is shown in Fig. 6. It is clear that the array's angular resolution is responsible for the broadening at low frequencies. Each line obviously corresponds to a ship and the long tail in frequency is clearly associated with the same ship. This point is followed up in section 4.4. Broadening effects can be seen at the top and bottom near forward and backward endfire. The curved lines on the right at top and bottom are artifacts caused by grating lobes beyond the design frequency (1500 Hz). The deep blue section is beyond the limit of the anti-aliasing filter.

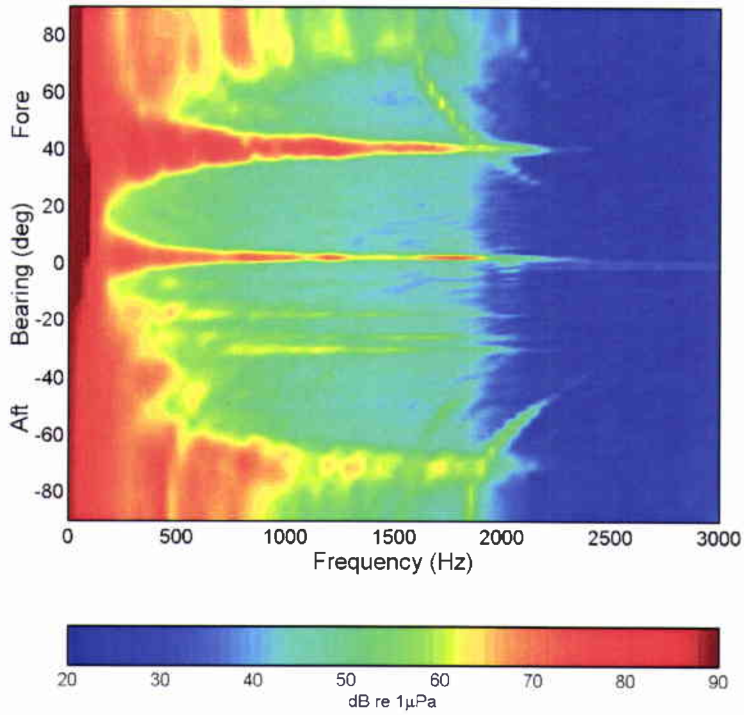

Figure 6 *Typical beamformed spectrum (time 60 min; calm day)*

4.3 Various statistics

By looking at the variation of noise in time (for each frequency and beam angle separately) one can differentiate various features. For instance, we can regard the noise to be composed of two frequency-dependent, directional components: a time invariant one from wind and distant ships, and a spiky one due to the sudden appearance and disappearance of local ships in the beam. We therefore expect the maximum to correspond to one or more of the local ships, but the (statistical) mode to correspond to the most likely value of the smooth background. In other words the probability distribution has a long tail corresponding to the rare but high intensity local ships. Other simple statistics are the mean, median and minimum. Although at this stage it is not clear what these represent exactly we will see that they are quantities that have real meaning in the context of understanding the background against which we try to detect a signal.

The maximum is shown in Fig. 7. The apparent discretisation of the peaks in angle in Fig. 7(a) is an artifact caused by the 5 minute gaps in reception.

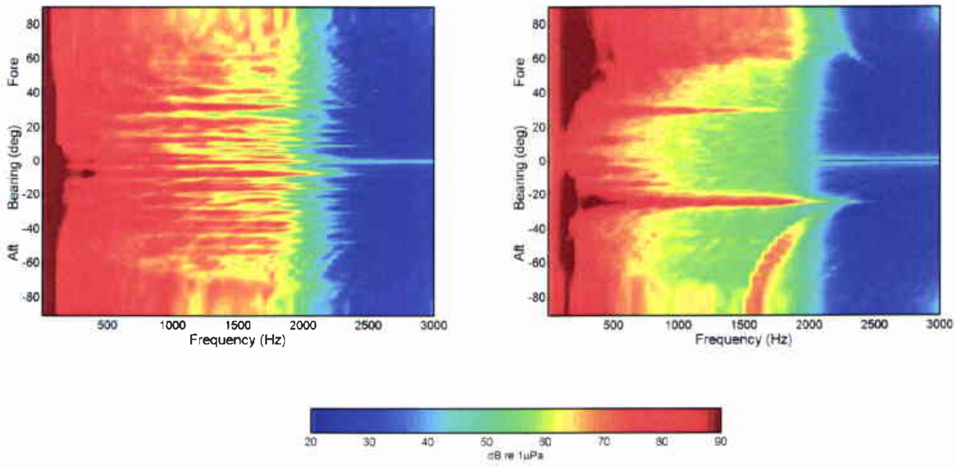

Figure 7 *Maximum intensity over time for (a) calm, (b) rough day.*

The mean and median are shown in Figs. 8 and 9. The values of the mean and median for the same day are surprisingly close considering the skewness of the distribution. Notice that on the rough day there are now one or two clear bottom reflected paths from the *Alliance* at about 72° and 65°. These correspond to the direct-bottom and the surface-bottom paths respectively with a stern to array separation of 600 m, water depth of 119 m and array depth of 43 m. Further reflections are precluded by the bottom critical angle. Note also that although NRV *Alliance* is a quiet ship from the point of view of engine noise it is not immune from producing a wide spectrum of 'hull slamming' and splashing sounds in high sea states.

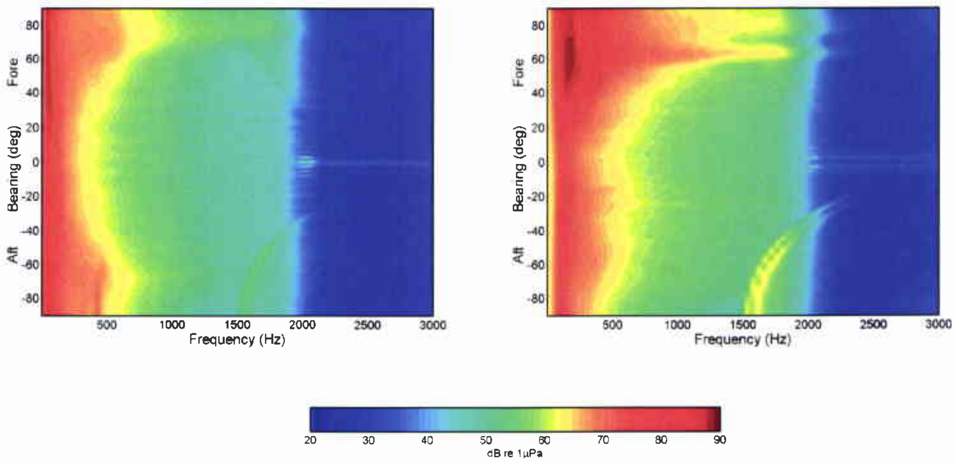

Figure 8 *Mean intensity over time for (a) calm, (b) rough day.*

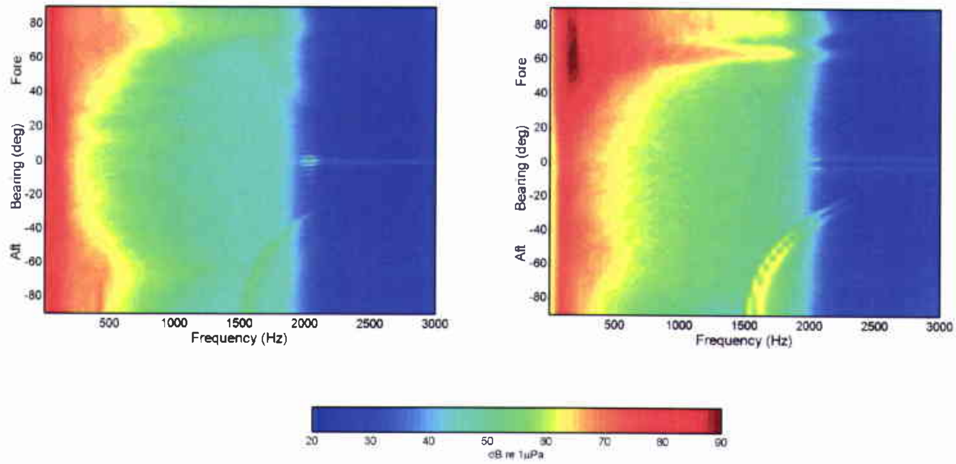

Figure 9 *Median intensity over time for (a) calm, (b) rough day.*

The minimum (Fig. 10) is interesting because although there is an overall difference of about 6 dB there is surprisingly little difference between the calm and the rough day, suggesting that there are times when the noise goes down to a floor value even in bad weather. On the assumption that this is a local noise source effect and not a propagation effect one could take advantage of it in a practical system by picking periods when the signal to noise is high before deciding to include them in the average. It is already well known that when the SNR fluctuates opportunities for detection are provided by the change in slope of the ROC curve (see e.g. [5]), but this effect is usually attributed to changes in the signal level against a steady background rather than changes in the background itself. The problem with a real system looking for real targets is that it cannot tell when the noise alone is weak since it only measures signal-plus-noise.

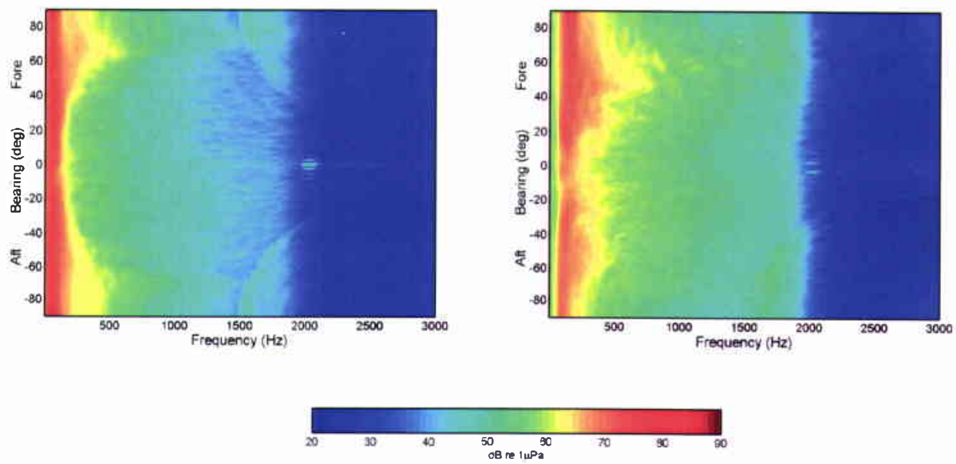

Figure 10 *Minimum intensity over time for (a) calm, (b) rough day.*

A contributing factor is that in bad weather many ships head for port or, at least shelter, where they do not make noise. The differences seen particularly in Fig. 7 are probably mainly due to this rather than poor propagation, although one cannot be certain. Similarly the satellite image [2] shows few ships on the rough day, but again there is the problem that they would be difficult to detect against a background of large waves, so one cannot be sure.

The mode, as the most likely value, would be appropriate to calculate since it corresponds to the diffuse background (of wind noise and distant shipping) with local ships extracted. Unfortunately the value with maximum probability has to be taken from a histogram whose definition, though rigorous, depends on an arbitrary bin size. Instead we therefore resort to a plot of the histogram (number of times an intensity falls in a set of bins) versus frequency. These are shown in the Appendix.

Summary plots of noise versus frequency for maximum, mean, median, and minimum are shown in Figs. 11 and 12. Each figure shows three steer angles: aft, broadside, and fore.

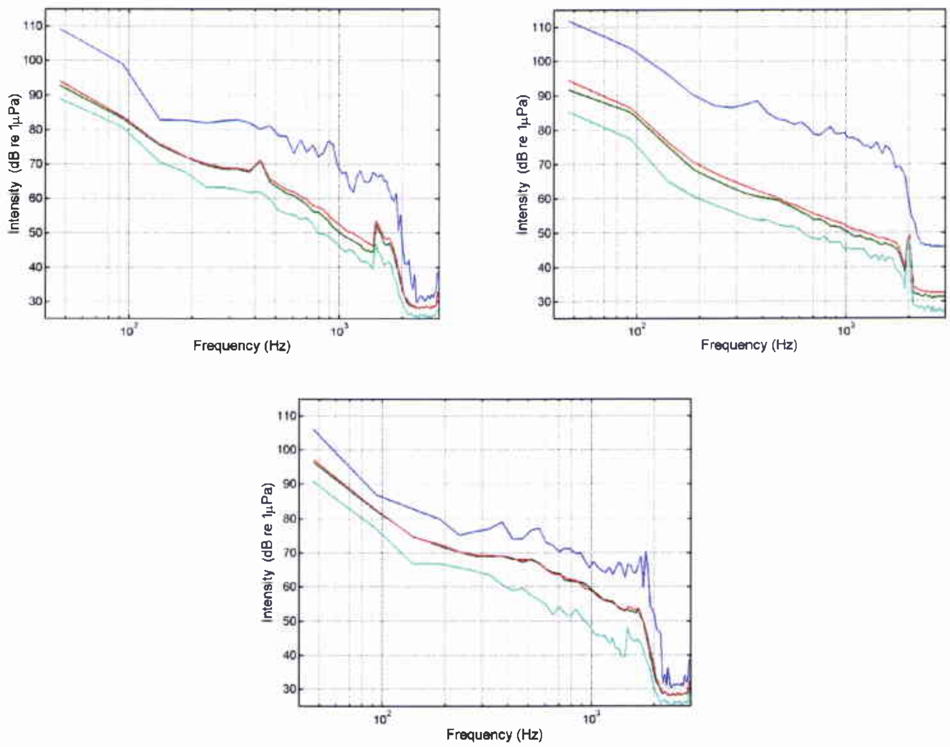

Figure 11 *Intensity vs frequency: aft, broadside, fore on calm day: Maximum (blue), Mean (red), Median (dark green), Minimum (cyan).*

An interesting point is the relative distance of the mean/median from the maximum and minimum remembering that the time series is already an averaged quantity. In Fig. 11(b) broadside we expect the mean to be closer to the minimum because of the rare loud events as ships pass through beams. A similar effect is seen in Fig. 11(a) probably caused by the ship at the bottom right of Fig. 3(a) crossing the endfire beam. The occurrence again in Fig. 12(a) for backwards endfire on the rough day is more puzzling, but the histograms in the Appendix show that this is again an isolated event i.e. one ship. In Fig. 12(c) the mean is nearer to the maximum than the minimum indicating that there are more frequent highs than lows. This can be attributed to the rare quiet intervals between hull 'slams'.

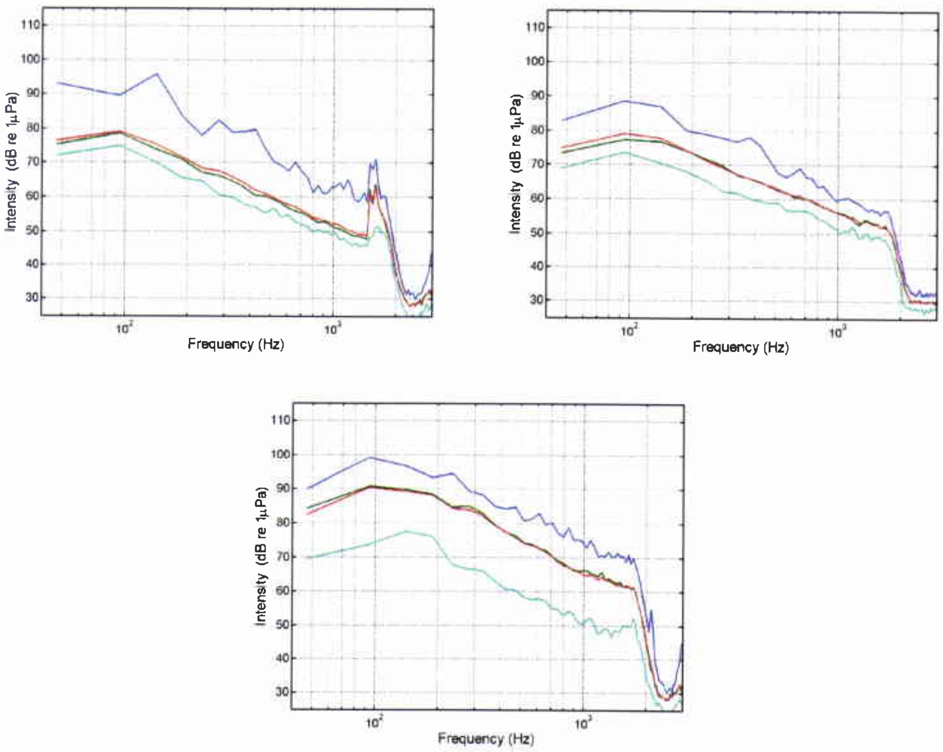

Figure 12 *Intensity vs frequency: aft, broadside, fore on rough day: Maximum (blue), Mean (red), Median (dark green), Minimum (cyan).*

In Fig. 11 a further interesting point is that between 50Hz and 2KHz *all* curves can be reasonably well approximated by a 20 log f fall-off. In the broadside case we know that the maximum is local individual ships and the law agrees with that assumed for shipping source strength in RANDI-3 [6]. Comparing the minimum curve (cyan) for broadside in Figs. 11 and 12 we see that the level rises by about 6 dB on the rough day. We also know that the minimum corresponds to wind and possibly distant ships. Since there are fewer local ships because of bad weather, by implication there are also fewer distant ships, and we can interpret this noise as wind-generated. Therefore this suggests that wind noise follows the same law in the 100 Hz to 2 KHz frequency range, and this agrees with measurements in [7].

Figures 13 and 14 show the same information as a function of steer angle. A more detailed look at the probability distributions is given in the Appendix. It is more obvious that an important difference between calm and rough is the sparsity of the shipping on the rough day. For this reason the noise is actually10 dB weaker on the rough day. The relative max, mean and min levels can be seen to change quite dramatically from forwards to backwards endfire.

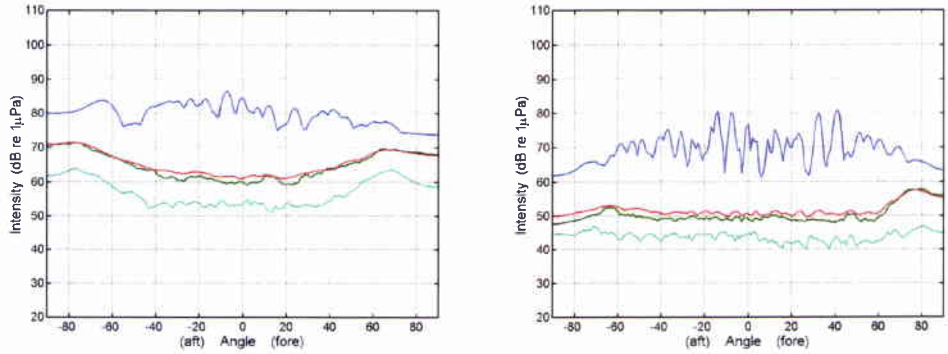

Figure 13 *Intensity vs beam angle: for frequency 500 and 1250Hz on the calm day: Maximum (blue), Mean (red), Median (dark green), Minimum (cyan).*

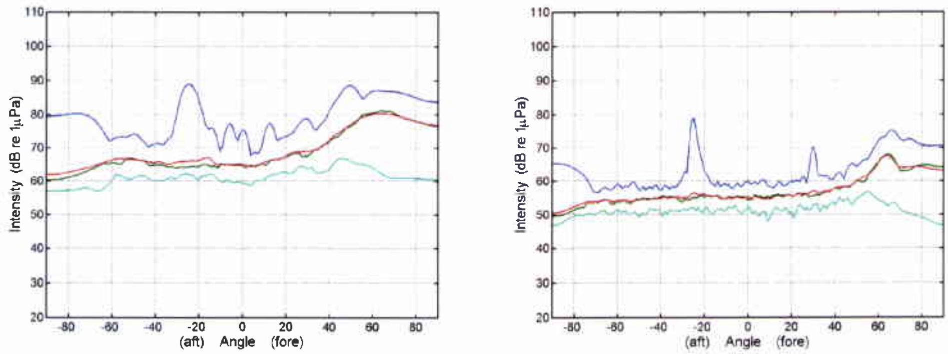

Figure 14 *Intensity vs beam angle: for frequency 500 and 1250Hz on the rough day: Maximum (blue), Mean (red), Median (dark green), Minimum (cyan).*

4.4 Implications for individual ships

If in Fig. 3(a) we pick out the intensity at the bearing and time corresponding to a single ship, e.g. -50° at t=0 through +30° at t=50 min etc we can interpolate between peaks to obtain a smooth maximum intensity vs bearing (actually aspect angle of the ship assuming it has the same constant heading as the *Alliance*) and frequency. In Fig. 15 we take the sequence of 7 ships from left to right reaching a red intensity level in Fig. 3(a). The 6th and 7th may well be the same ship performing a maneouvre that results in the upside down 'ν' shape on thebearing-time plot between 200 and 250 minutes. The ships can easily be identified in the following plots by their start and end angles.

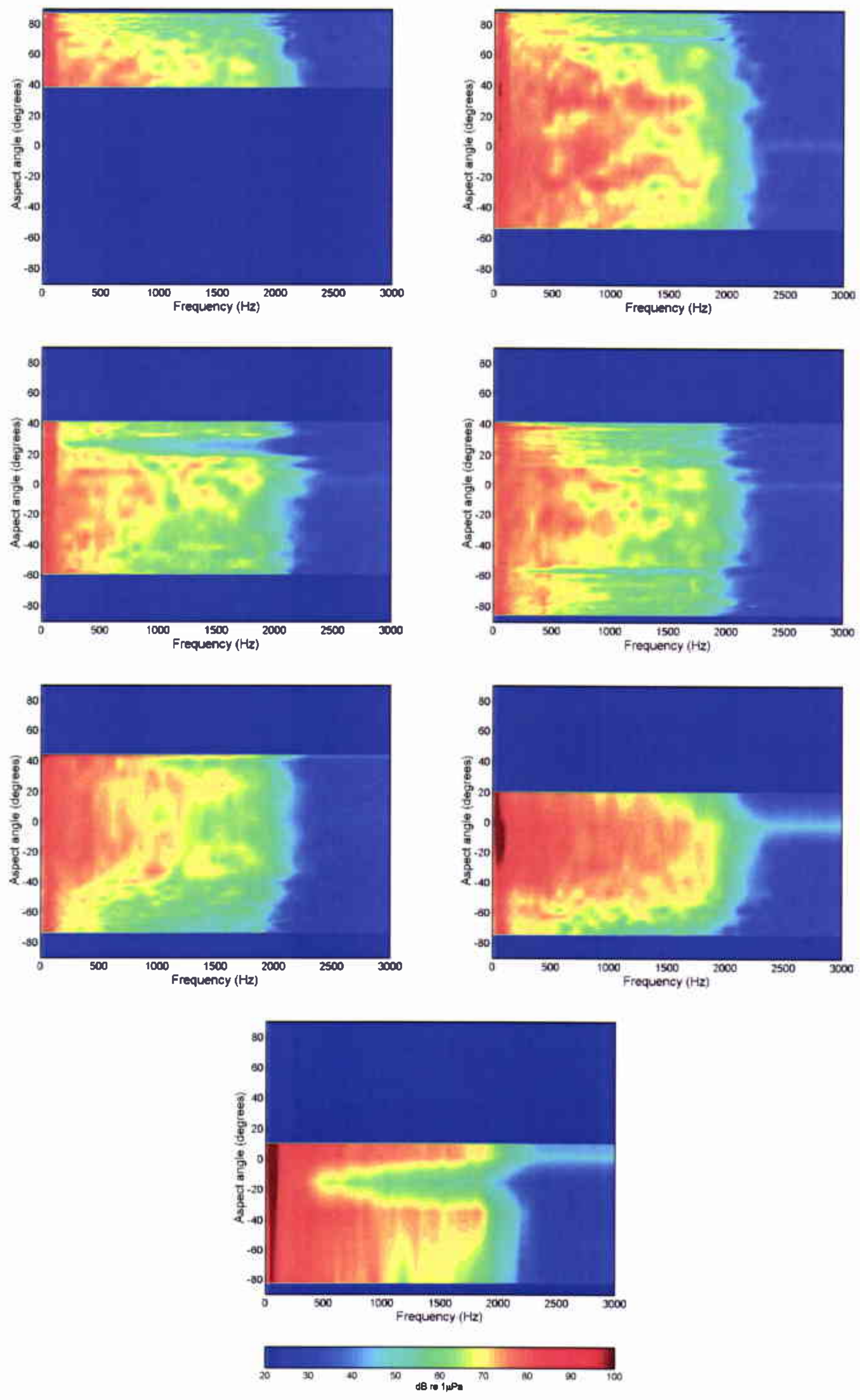

Figure 15 *Interpolated spectra vs aspect angle for 7 individual ships assumed on a parallel course to the array. Each 'ship' corresponds to one of the intermittent brown/red lines in Fig 3(a).*

We can now look at the spectrum in isolation by taking the average over angle for each ship as shown in Fig. 16. Not surprisingly the frequency dependence is again 20 log f between 50 Hz and 2 KHz.

The absolute intensity also varies because the ship range changes as $r = r_{cpa} \sec\theta$, again assuming parallel tracks. At ranges of only a few kms one expects intensity to fall off according to 'mode stripping' i.e. 15 log r , so in addition to any genuine source aspect effects (i.e. looking at the ship's stern in the fore direction and bow in the aft direction) we have a 15 log(sec θ) component due to transmission loss. Compensating for this raises levels by 0.93 dB at ±30° and by 4.5 dB at ±60°. A modified plot of spectra is shown in Fig. 17. Note that although we know the ship must have changed range as it passed we do not know its absolute range, so the dB scale is only absolute in the broadside direction. We can estimate the range from the bearing rate at broadside by assuming that the speed is 12 kt. By inspection of Fig. 3(a) their bearing rate is between 1.4 and 1.9 deg/min so their ranges at cpa are 12.5 km. Of course, one could perform much more sophisticated propagation modelling; here the intention is merely to show that individual ships, with their frequency and angle dependence, can be separated from the smooth background of wind and distant shipping, with it's own frequency and angle dependence.

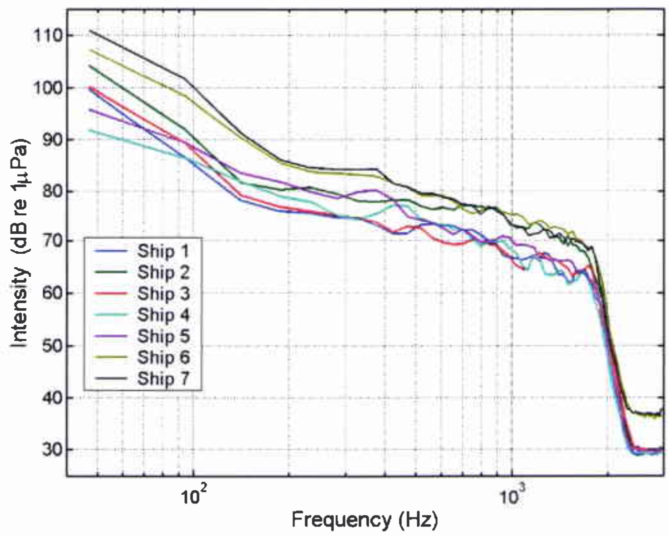

Figure 16 *Individual ship spectra uncompensated for range*

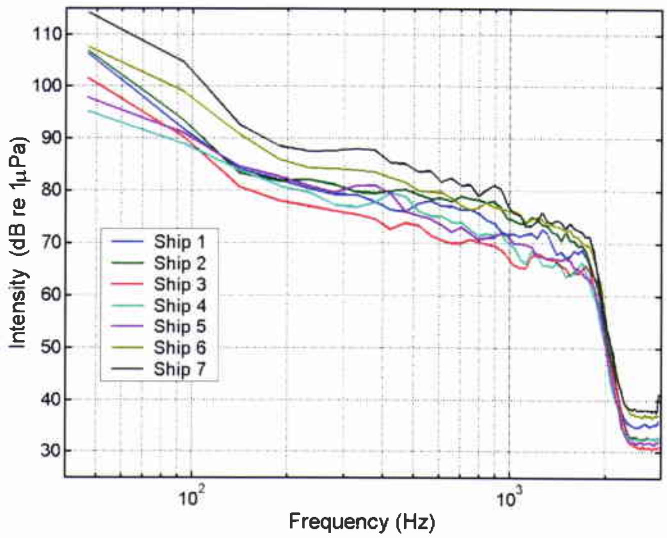

Figure 17 *Individual ship spectra compensated for range*

5 Conclusions

- During MAPEX2000 directional ambient noise data were gathered with a horizontal array while travelling more or less parallel to a dense shipping lane south of Sicily. The original intention was to compare these measurements with noise predictions using shipping and wind information gathered from commercial satellites. The purpose of this report was to look at measured noise alone.

- A simple technique was proposed and used for separating the nearby shipping from the more diffuse wind noise and distant shipping. In this way one can obtain a directional spectrum for the diffuse noise background. It is clear from e.g. Fig. 3 that in sites such as this the nearby shipping changes the directionality beyond recognition in 20 min or less.

- The receiving ships' own radar could provide good enough information to predict range and bearings for the acoustically nearby shipping. The update rates for commercial satellite SAR (with or without processing time) is usually far too slow to provide this information. On the other hand the satellite coverage area is greater and could possibly satisfy the need for acoustically distant shipping whose geometry changes less dramatically with time.

- By always choosing the bearing for an individual ship it is possible to map out its spectrum as a function of aspect angle. In these cases there was not much variation in spectral shape from ship to ship.

- More sophisticated modelling of wind, nearby and distant shipping is possible, but no attempt was made in this study because of the unknown ship ranges and source levels. Models such as RANDI-3 already include a source spectrum whose shape is very similar to those measured here (Figs. 16, 17). The actual level is parameterized in terms of the ship length and crucially the ship speed.

- An interesting possibility from the point of view REA and tracking (though not so far tried) is first to localize the nearby ships and then to use them as sound sources of opportunity for geoacoustic inversion. Using the beamformed data there is usually only one strong ship at any instant so a matched field processing algorithm, or some such, ought to perform reasonably well.

- An interesting point found with the temporal statistics of the measured noise was that the minimum (as a function of angle and frequency) appeared not to depend very much on the weather, implying that there could be a benefit in paying closer attention to the statistics of the noise on a time scale of a few seconds. Perhaps in rough weather it is still possible to find relatively quiet conditions in between local waves.

- *Alliance* self-noise could be detected through the bottom reflected paths between 65° and 70°. This is mainly hull-slamming and associated spray noise which is much worse on the rough day. The weak dependence on angle elsewhere in the plots demonstrates that the weather-independent minimum (mentioned above) is not simply self-noise.

References

[1] MAPEX2000 Cruise SACLANTCEN CD-54.

[2] Askari, F., Zerr, B. An automatic approach to ship detection in spaceborne synthetic aperture radar imagery: an assessment of ship detection capability using RADARSAT. SACLANTCEN SR-338, 2000.

[3] Scrimger, P., Heitmeyer, R.M., Boulon, P. A computer model of merchant shipping in the Mediterranean Sea. SACLANTCEN SR-164, 1960.

[4] Troiano, L., Guerrini, P., Barbagelata, A. SACLANTCEN towed and vertical array system characteristics. SACLANTCEN M-117, October 1995.

[5] Urick, R.J. Principles of Underwater Sound for Engineers. Mc Graw-Hill, NY, 1967.

[6] Breeding, J.E., Pflug, L.A., Bradley, M., Hebert, M., Wooten, M. RANDI 3.1 User's Guide. Naval Research Laboratory Report No. NRL/MR/7176—94-7552, 1994.

[7] Kuperman, W.A., Ferla, C. A shallow water experiment to determine the source spectrum level of wind-generated noise. *Journal of the Acoustical Society of America*, 77, 1985:2067.

Annex A: Measured Probability Distributions

Figures A1-4 are equivalent to Figs 11-14 in the main text. They are histograms in which colour indicates the number of times (out of 52 on the calm day or 18 on the rough day) an intensity is found for each frequency and bearing. By inspection one can see the various statistics, such as, minimum, maximum, mean, median, and these can be checked against the curves for these quantities in Figs 11-14. The superimposed black line here is the mean.

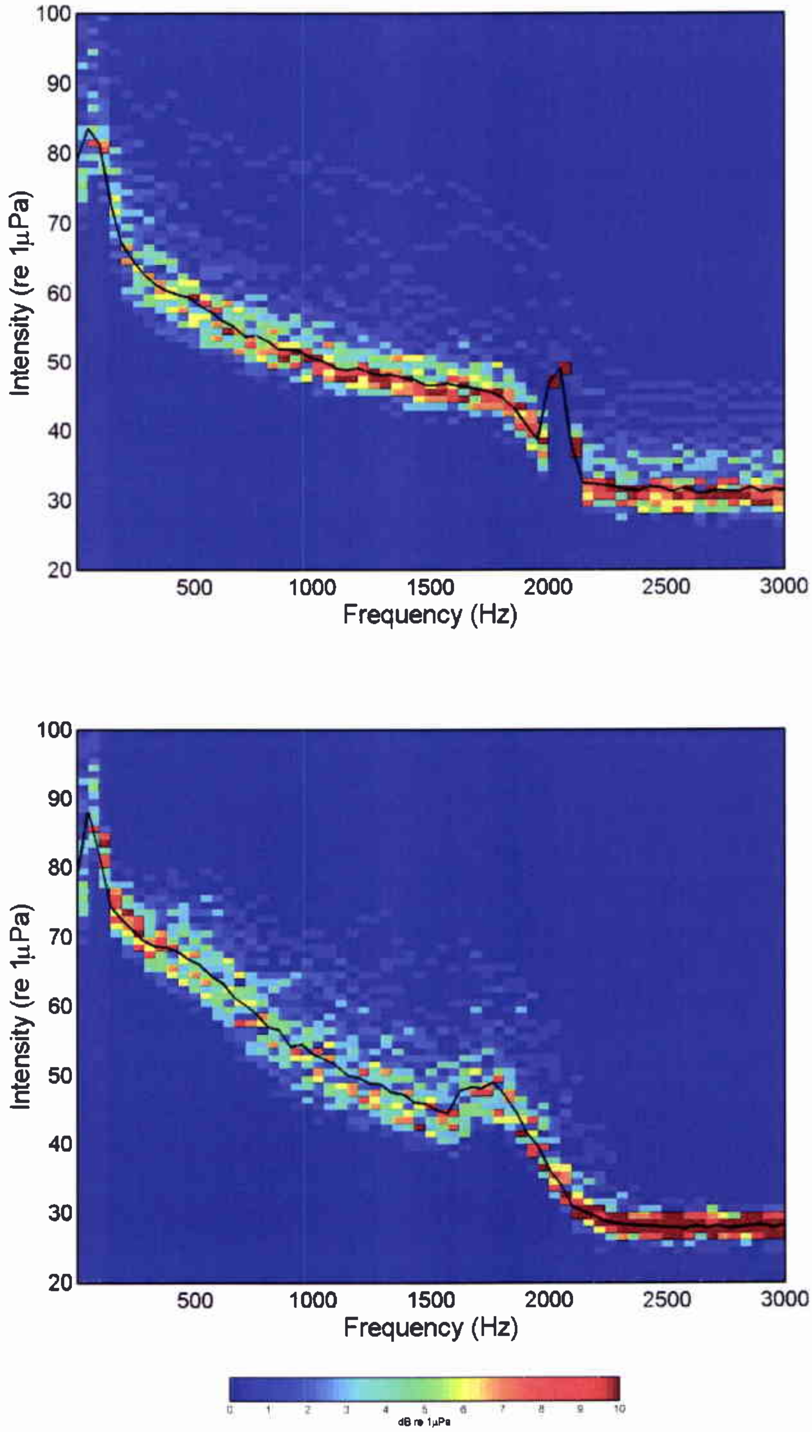

Figure A1 *Histograms vs Intensity and Frequency for calm day (a) broadside, (b) 60° forward.*

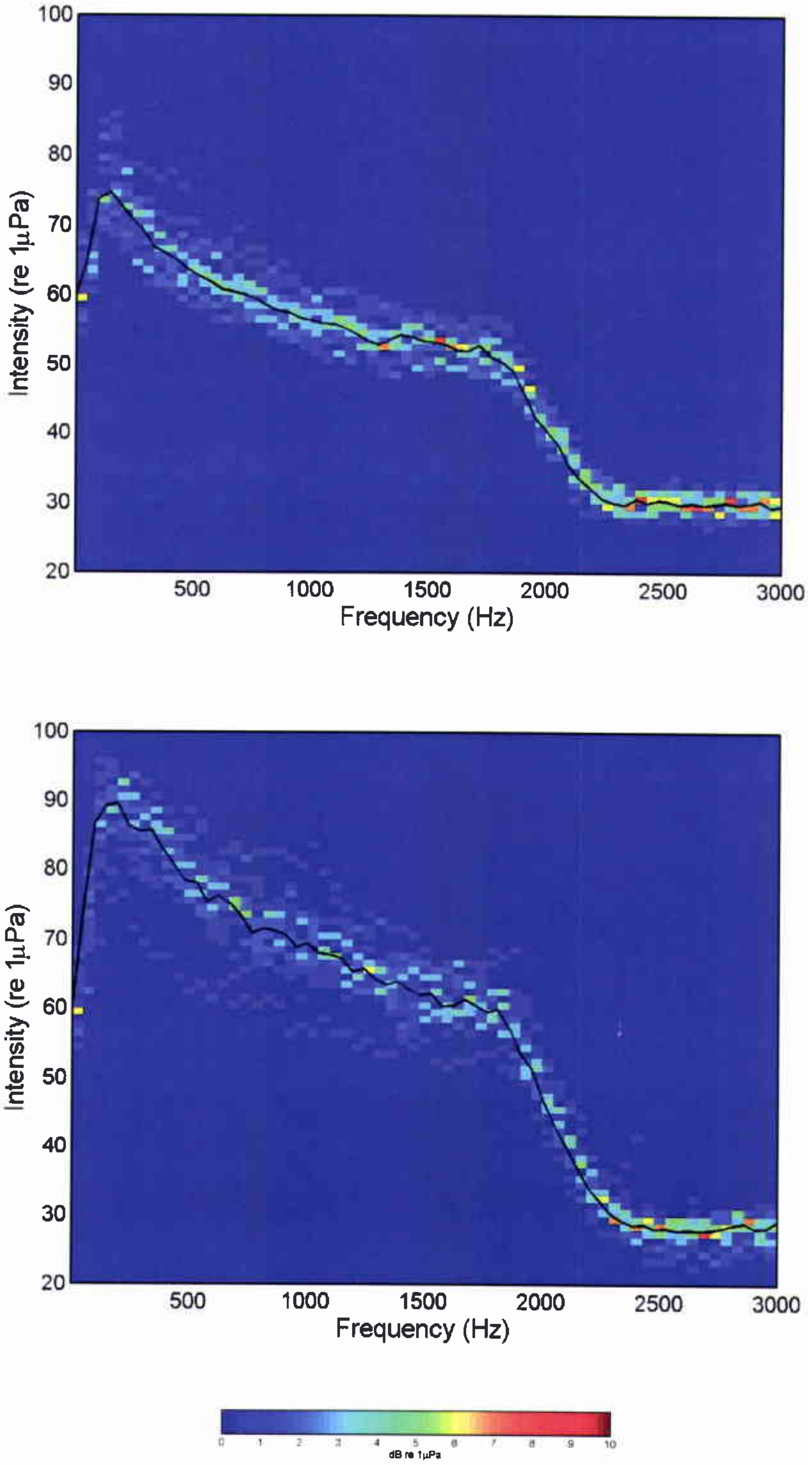

Figure A2 *Histograms vs Intensity and Frequency for rough day (a) broadside, (b) 60° forward.*

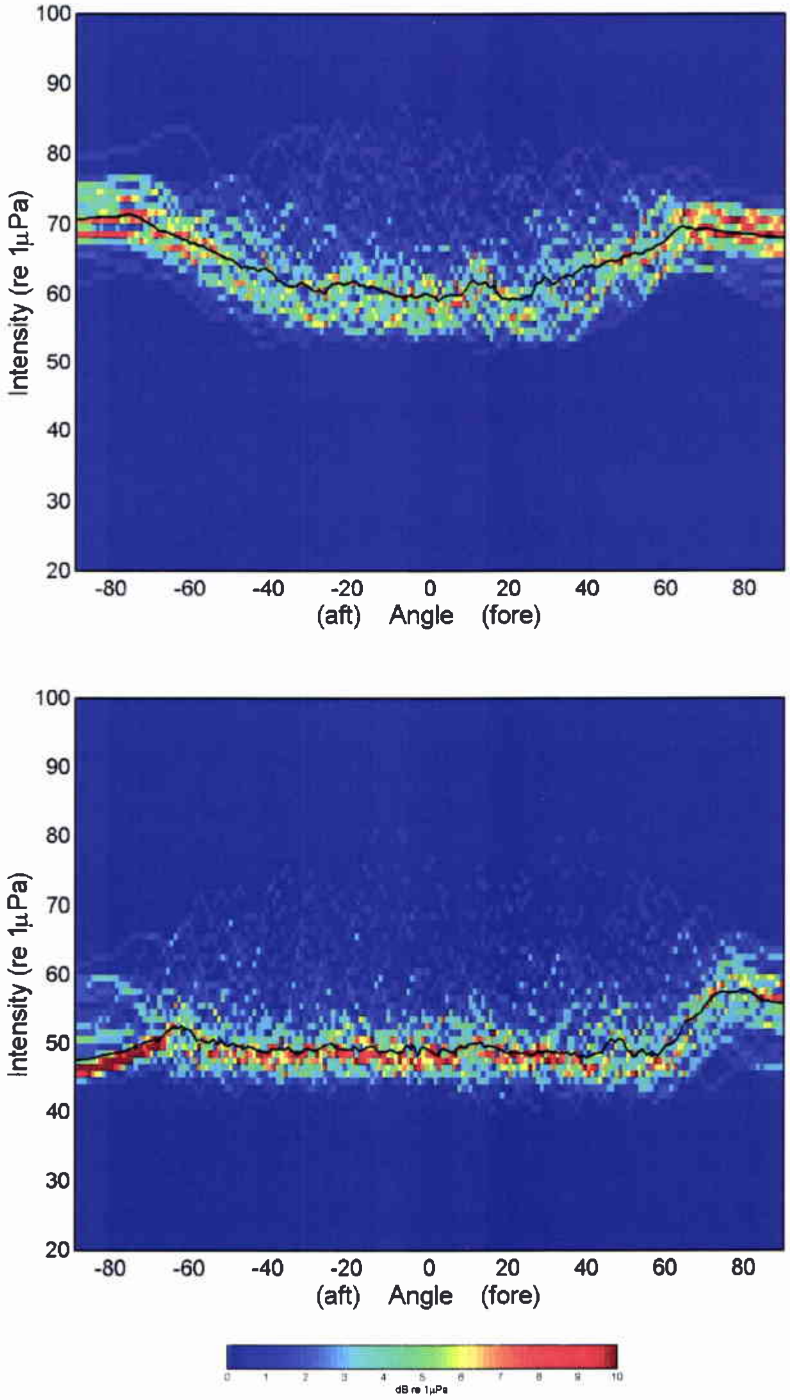

Figure A3 *Histograms vs Intensity and Bearing for calm day (a) 500Hz, (b) 1250Hz.*

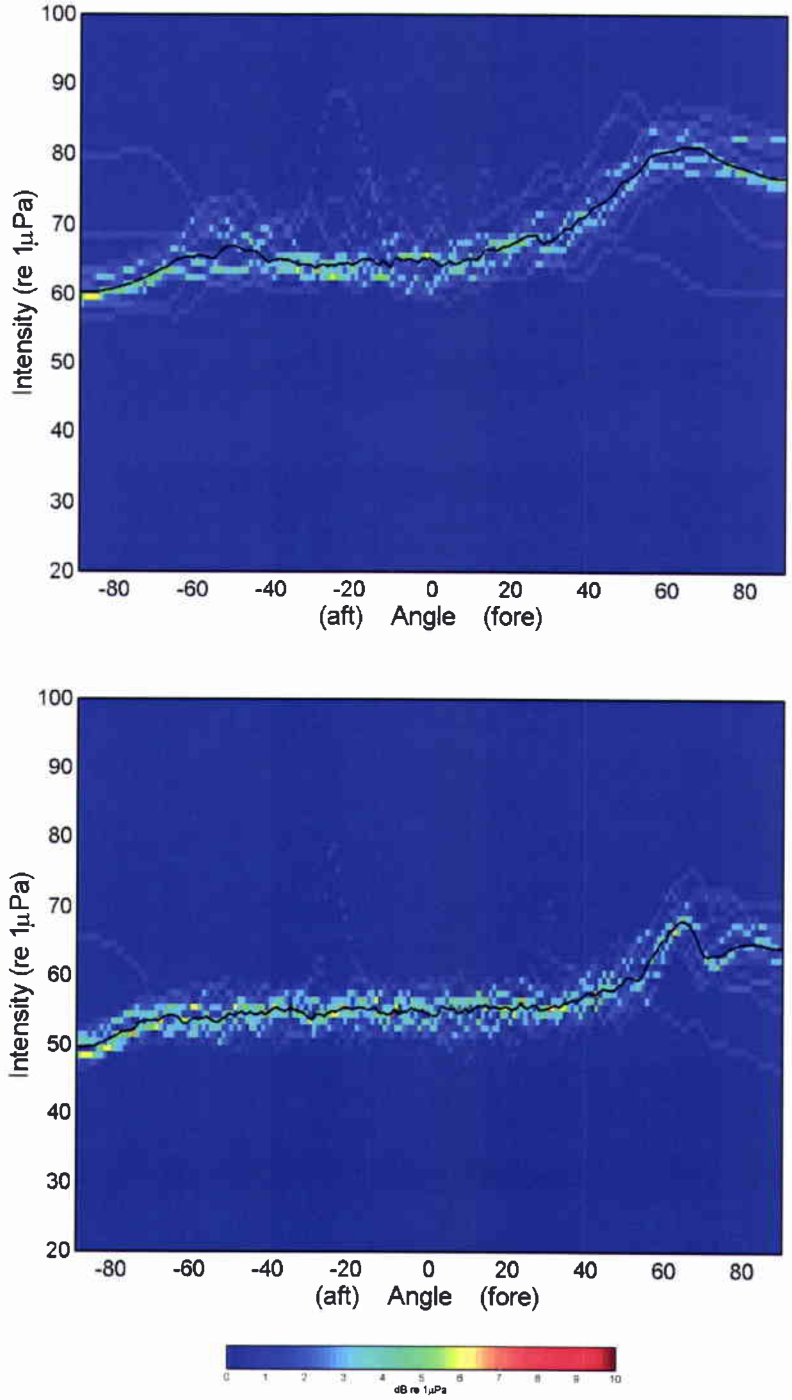

Figure A4 *Histograms vs Intensity and Bearing for rough day (a) 500Hz, (b) 1250Hz.*

Report no. changed (Mar 2006): SM-391-UU

Document Data Sheet

Security Classification	Project No.
UNCLASSIFIED	01-B

Document Serial No.	Date of Issue	Total Pages
SM-391	November 2002	34 pp.

Author(s)

Harrison, C.H.

Title

Noise measurements during MAPEX2000

Abstract

During MAPEX2000 some simultaneous ambient noise measurements with an HLA and satellite SAR images were collected. The aim was to predict shipping and wind noise from the satellite radar and to compare results with acoustic measurements. This report takes the acoustic data alone and investigates differences in noise directionality and shipping densities in fair and rough weather conditions. Directionality and various statistics are studied as a function of frequency and time (several hours). In addition, picking one ship at a time it is possible to study its aspect dependence as it passes the HLA.

Keywords

Ambient noise, wind noise, shipping noise, beam-forming, HLA, noise directionality

Issuing Organization

North Atlantic Treaty Organization
SACLANT Undersea Research Centre
Viale San Bartolomeo 400, 19138 La Spezia, Italy

[From N. America: SACLANTCEN (New York) APO AE 09613]

Tel: +39 0187 527 361
Fax:+39 0187 527 700

E-mail: library@saclantc.nato.int

Report no. changed (Mar 2006): SM-391-UU

The SACLANT Undersea Research Centre provides the Supreme Allied Commander Atlantic (SACLANT) with scientific and technical assistance under the terms of its NATO charter, which entered into force on 1 February 1963. Without prejudice to this main task - and under the policy direction of SACLANT - the Centre also renders scientific and technical assistance to the individual NATO nations.

SACLANT Undersea Research Centre
Viale San Bartolomeo 400
19138 San Bartolomeo (SP), Italy

tel: +39 0187 527 (1) or extension
fax: +39 0187 527 700

e-mail: library@saclantc.nato.int

NORTH ATLANTIC TREATY ORGANIZATION